

BUCKLING OF STEEL PLATES AT ELEVATED TEMPERATURES: THEORY OF PERFECT PLATES VS FINITE ELEMENT ANALYSIS

C. Maraveas, T. Gernay & J.M. Franssen, *University of Liege, Belgium*

ABSTRACT

The local buckling capacity of fire exposed thin-walled steel cross sections is affected by the reduction in strength and stiffness due to elevated temperatures and the amplitude of the initial local imperfections. Several researchers have proposed design methods to calculate the capacity of the plates (i.e. web and flanges) that compose these steel members at elevated temperatures, but they used different shapes of steel plates (sides ratio a/b) and different amplitudes of local imperfections. This variability in hypotheses happens because there is no clear provision defining the numerical modeling procedure for fire design of steel plates in the codes (European or US). According to the theory of perfect plates, the critical load depends of the shape of the rectangular plate (e.g. the sides ratio a/b) and the corresponding buckling mode (number of half waves), the boundary and the loading conditions. This paper reviews the existing code provisions and compares the existing design models and their assumptions for thin-walled steel cross sections. Elements of the theory of perfect plates are presented. Parametric finite element analyses are then conducted on isolated steel plates at elevated temperatures to investigate the effect of the plate shape (a/b ratio) and imperfections (amplitude and number of half wave lengths). From the analysis, the governing parameter will be estimated (a/b vs imperfections) for simulation of isolated flanges and webs. Finally, recommendations for the numerical modeling of steel plates at elevated temperatures are proposed.

1. INTRODUCTION

The use of slender steel sections, i.e. sections made of thin steel plates, has increased in recent years because they provide excellent strength to weight ratio; this trend has also been favoured by the development of higher steel grades. Yet, a major issue with slender sections is local buckling that may occur in zones subjected to compression: in the flange under compression for elements in bending and in the web for elements in compression. In very deep sections, shear can also trigger local buckling in the web if it is too slender. Furthermore, past fire accidents have demonstrated local buckling failures in structural members with slender cross sections, like in WTC 5 [1] and Broadgate fire [2].

To take local instabilities into account, several design methods have been proposed by researchers based on finite element analyses of isolated plates [3], [4], [5], [6] or analytical methods [7]. As the current codes do not include a specific method for the calculation of the capacity of such structural members at elevated temperatures, the ambient temperature methods of EN 1993-1-5, 2006 [8] and AISC, 2005 [9] can be used in conjunction with elevated temperature

material models from EN 1993-1-2, 2005 [10] or AISC, 2005 [9] respectively. A comparison of the plate capacity predicted by different proposed models, whether based on design codes or numerical analyses, is showed in Figure 1. The horizontal axis on the plot is the elevated temperature plate slenderness (Eq. 5) and the vertical axis is the strength reduction due to local buckling. Although these models give similar trends, the discrepancy in quantitative results is significant with a ratio in the order of 2 between the extremes. Table 1 shows the governing parameters (i.e. assumptions) used in the models based on numerical analyses. The parameters a , b and t are the length, width and thickness of the plate, respectively. It can be seen that different authors assumed different values for these parameters, which naturally lead to different results. The results are affected by the amplitude of the initial local imperfections, by the geometry of the local imperfections (number of half-waves) and by the dimensions of the plate (ratio a/b) [11]. The effect of the amplitude of the initial local imperfections is discussed in another study [12]. This paper presents an investigation on the influence of the geometry of the local imperfections (number of half-waves) and the

dimensions of the plate (ratio a/b). Considering the theory of perfect plates and numerical results of simulations on isolated plates, recommendations are made for the geometry of the local

imperfections (number of half-waves) and the dimensions of the plate (ratio a/b) for the numerical modeling of steel plates at elevated temperatures.

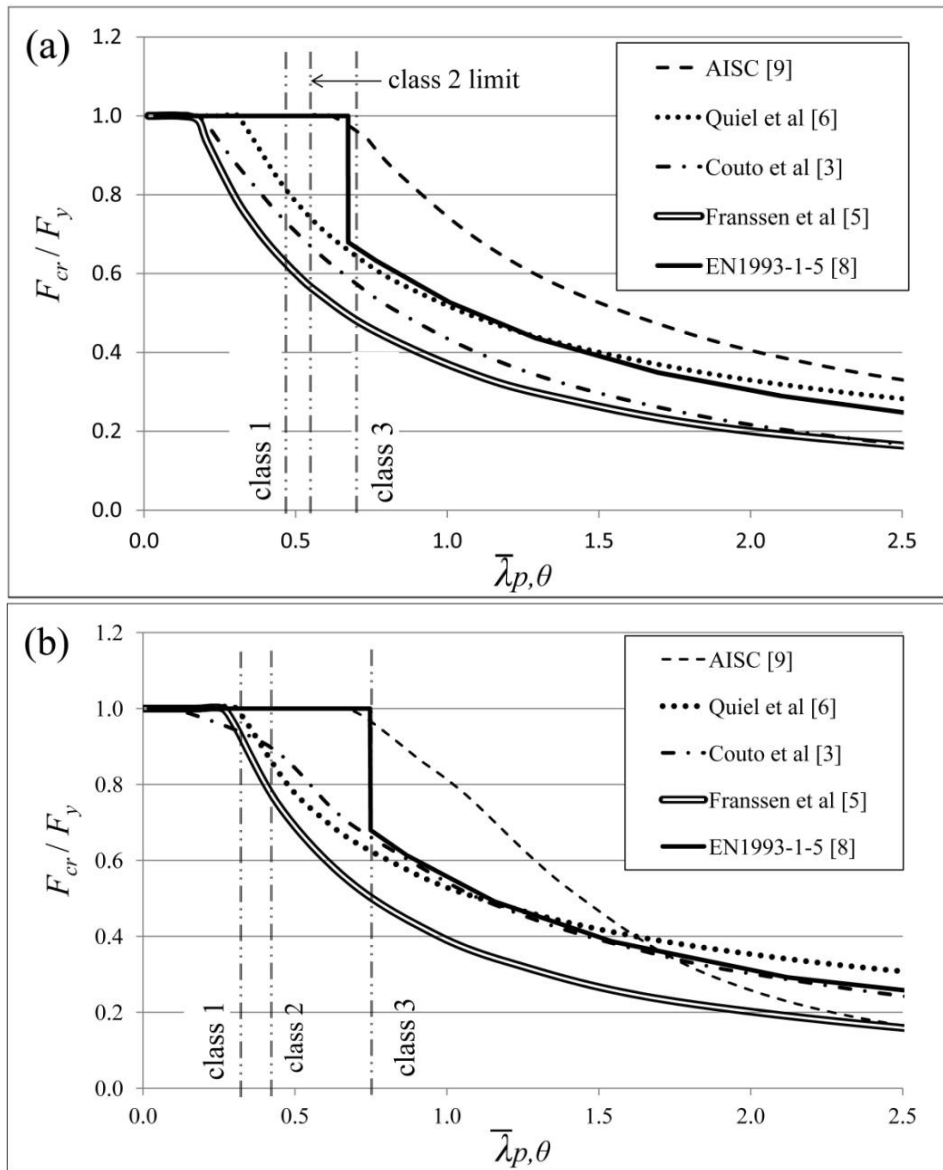


Figure 1. Comparison of proposed design and code methods for capacity of slender plates at 500 °C (S235), (a) for stiffened plates (web) and (b) for unstiffened plates (flange).

Table 1. Governing analysis parameters used in the numerical simulations by different authors.

Reference	a/b	Number of half-waves	Amplitude of imperfections
Franssen et al, 2014 [5]	flange: 2 web: 1	1	flange: $b/50 = 0.020 b$ web: $b/200 = 0.005 b$
Couto et al, 2014 [3]	4	flange: 1, web: 4	flange: 80% $b/50 = 0.016 b$ web: 80% $b/100 = 0.008 b$
Quiel et al, 2010 [6]	5	flange: 3, web: 5	flange: 0.156 t web: 0.100 t

2. BUCKLING OF PERFECT PLATES

According to the theory of buckling of plates [13] the plate buckling governing equation of a plate in in-plane compression is:

$$D\nabla^4 w + N_{xy}w_{,xy} = 0 \quad (1)$$

where D is the bending stiffness of the plate, w is the out-of-plane displacements, N_{xy} is the in-plane load and $w_{,xy}$ is the in-plane displacement (Figure 2).

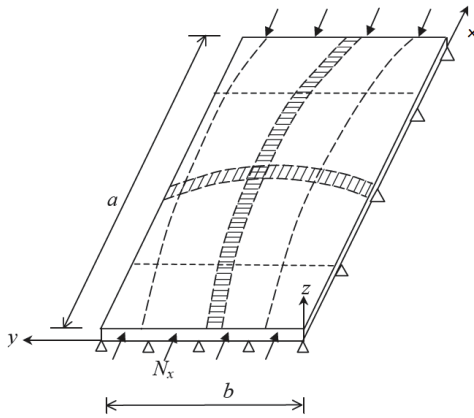


Figure 2. Typical plate under in-plane compression simply supported in four sides.

For long rectangular plates, Equation (1) can be reformulated as [14]:

$$\sigma_{cr} = k \frac{\pi^2 E}{12(1-\nu^2)(b/t)^2} \quad (2)$$

Where σ_{cr} is the critical stress, k is the plate buckling coefficient, E and ν are the modulus of elasticity and the Poisson ratio of the elastic material, b is the width of the plate and t is the plate thickness.

The plate buckling coefficient k depends on the applied boundary conditions. When the plate is short in the direction of the compressive stress, there exists an influence in the critical buckling stress due to the fact that the buckled half-waves which take integer values are forced into a finite length plate (Figure 3). Therefore for short plates, the plate buckling coefficient is also a function of the size of the plate (ratio a/b) and the number of half-waves m (Figure 4).

From Figure 4, for 4 sides simply supported plate, $a/b=m$ gives safe result (i.e. minimum value of k) and for 3 sides simply supported plate, $a/b>4$ and

$m=1$ is giving safe results. This preliminary conclusion applies to perfect plates.

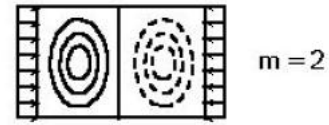
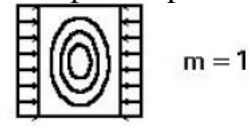


Figure 3. Different buckling modes (m is the number of half-waves) for different a/b ratios of 4 sides simply supported plates

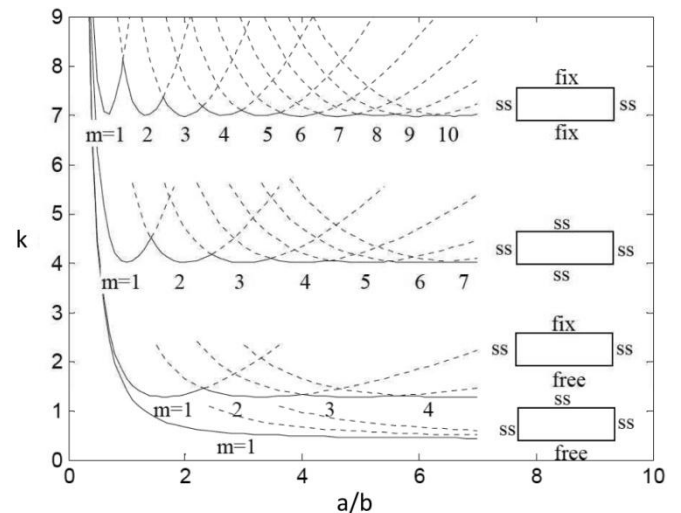


Figure 4. Buckling reduction factor for plates in compression as function of the shape of the plate a/b , the boundary conditions and the number of half-waves m [13].

3. BUCKLING OF IMPERFECT PLATES

As with all steel structures, plate panels contain residual stresses from manufacture and subsequent welding into plate assemblies, and are not perfectly flat (they have imperfections). The previous discussions (Section 2) about plate panel behaviour all relate to an ideal, perfect plate. As shown in Figure 5 these imperfections affect the behaviour of actual plates. For a slender plate the behaviour is asymptotic to that of the perfect plate and there is little reduction in strength (Figure 5a and 5c) as occurs elastic buckling and plastic

deformations appear at post buckling stage. For plates of intermediate slenderness (which frequently occur in practice), an actual imperfect plate will have a considerably lower strength than

that predicted for the perfect plate (Figure 5b and 5c).

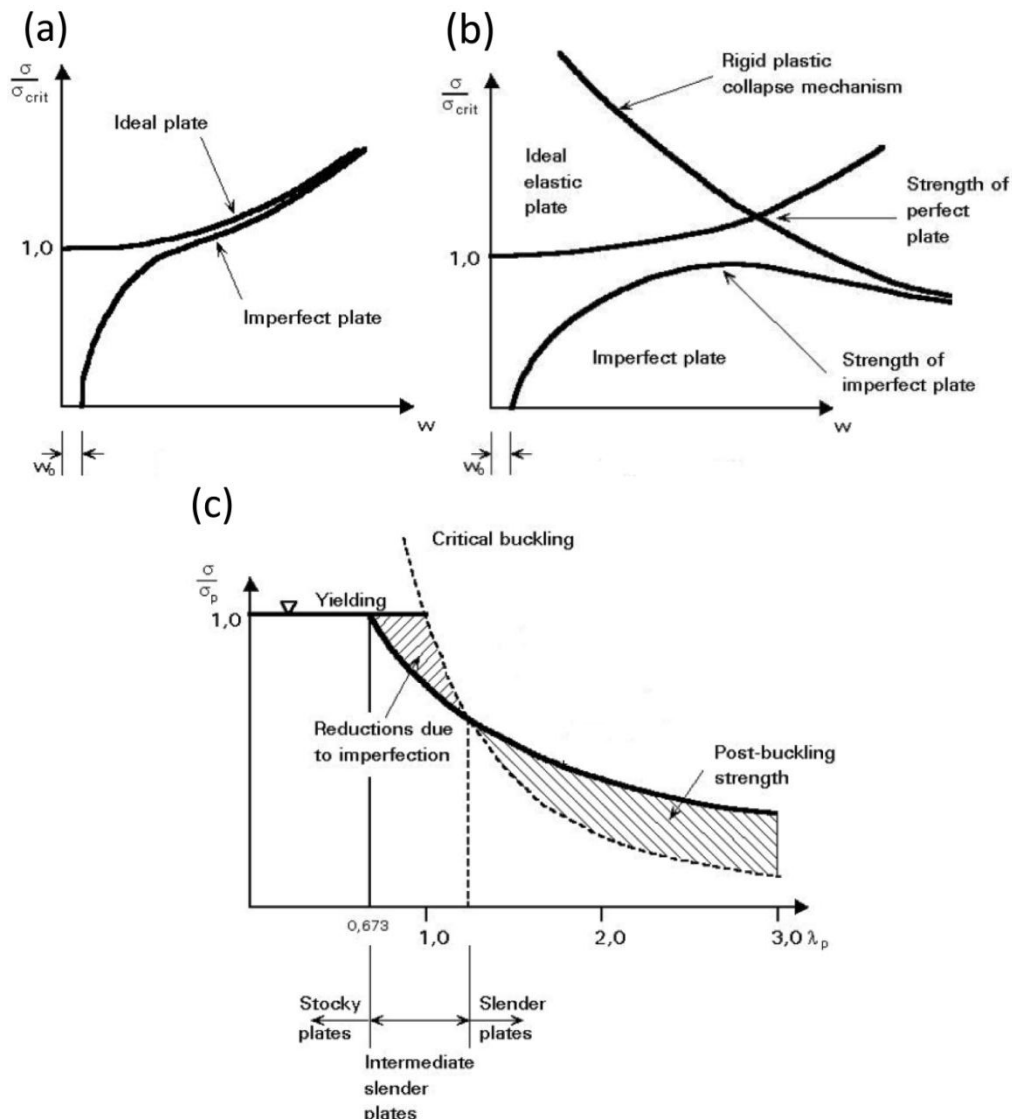


Figure 5. Effect of imperfections on plates of different slenderness in compression [16] (a) slender plates, (b) intermediate slender plates and (c) relationship between plate slenderness and strength in compression.

4. FINITE ELEMENT SIMULATIONS OF STEEL PLATES AT ELEVATED TEMPERATURES

In order to assess the effect of different dimensions (a/b ratio) and imperfection shape (number of half waves), finite element analyses of isolated plates are performed using the nonlinear finite element software SAFIR[®] [17-18]. The considered imperfection amplitude was $b/200$ as defined in [12]. The residual stresses are not considered as their effect is minor at elevated temperatures [19]. All analyses were performed at 550 °C. Two numerical models were used for

parametric analysis for different a/b and number of half-waves of imperfections. The first model (Figure 6(a)) is simply supported at all 4 sides; it is simulating a stiffened plate (equivalent to a web). With $a/b=1$, 400 shell elements are used based on convergence verification (Figure 7). For the parametric analysis when the ratio a/b is modified, the element size is kept the same so that the number of elements is equal to $400 \cdot (a/b)$. Imposed displacements are applied in the x direction at one side whereas the opposite side is restrained in the same direction. The lateral sides are free to expand in the y -direction, to allow unrestrained Poisson effect. The local

imperfections are applied in m half-wave ($n = 1$) following the Eq. (3):

$$w(x, y) = w_0 \sin\left(\frac{m\pi x}{a}\right) \sin\left(\frac{n\pi y}{b}\right) \quad (3)$$

where w_0 is the local imperfection amplitude.

The second finite element model is unstiffened (equivalent to a flange), simply supported on three sides (Figure 6(b)), with aspect ratio a/b and $400 \cdot (a/b)$ shell elements used after convergence verification. The local imperfections are applied in m half-waves ($n = 1$) following the Eq. 4:

$$w(x, y) = w_0 \sin\left(\frac{m\pi x}{a}\right) \sin\left(\frac{n\pi y}{2b}\right) \quad (4)$$

In order to assess plates of different slenderness, the thickness is modified to get different values of slenderness calculated according to Eq. 5 from EN 1993-1-5 [8]:

$$\lambda_{p,\theta} = \frac{b/t}{28.4\epsilon\sqrt{k_\sigma}} \quad (5)$$

where k_σ is a factor considering the applied boundary conditions defined in EN 1993-1-5 [8] and ϵ has been taken for elevated temperatures from the equation:

$$\epsilon = \sqrt{\frac{k_{E,\theta}}{k_{y,\theta}}} \sqrt{\frac{235}{f_y}} \quad (6)$$

where $k_{E,\theta}$ and $k_{y,\theta}$ are the reduction factors of Young's modulus and yield strength respectively for temperature θ .

The yield strength is taken as 235 MPa for both plates.

As critical force, the maximum total reaction due to the applied displacement is considered.

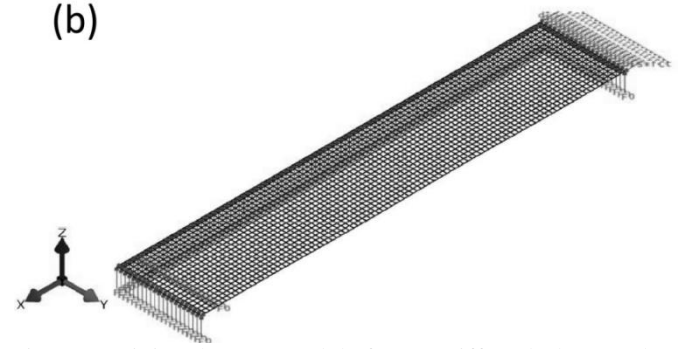
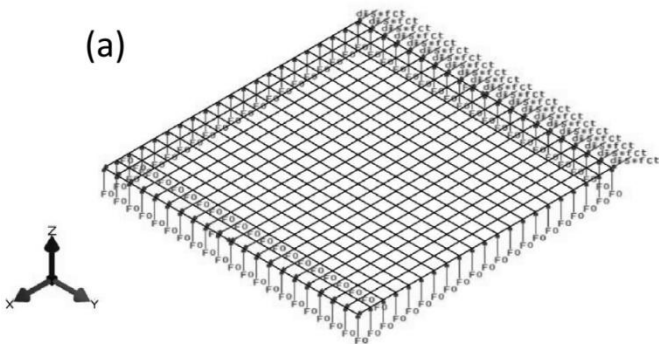


Figure 6. Finite element models for (a) stiffened plate (web) with $a/b=1$ and 400 elements and (b) unstiffened plate (flange) with $a/b=5$ and 2000 elements.

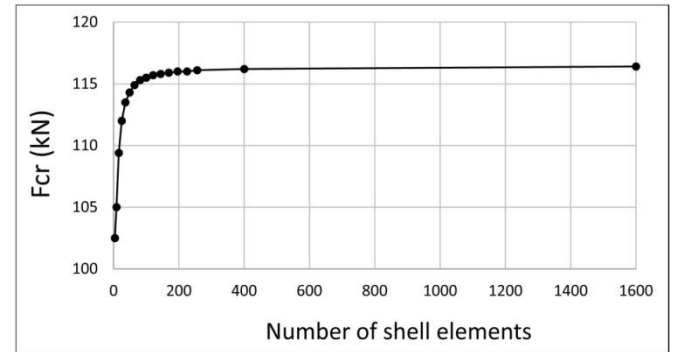


Figure 7. Convergence verification for square plate with $a = b = 0.4$ m under axial compression.

5. SIMULATIONS RESULTS

The results of the parametric analysis for the stiffened model (web) are presented in Figure 8(a). The convergence to the lower (safe) buckling load occurs for $m = a/b$, as expected from the theory of perfect plates. Yet, it is also observed that the buckling load remains at the minimum value for $m = a/b + 1$ (e.g. $m = 3$ when $a/b = 2$). For larger values of m (relative to a/b), the buckling load increases. The effect of a/b and m may affect the buckling load by up to 25%. (13)

Figure 8(b) shows the results obtained for two additional configurations: with a very small amplitude of imperfections ($b/2000$) and with fixed rotation along the x axis on the two lateral edges. These two configurations do not reach the minimum value of buckling load for the same value of m . When imperfections equal with $b/2000$ are considered, the analysis is giving safe results only for $m = a/b$, as the plate converges to the perfect plate due to very small imperfections. When the side rotations are fixed, the minimum buckling load is for $m = a/b + 1$, a result expected from the perfect plates theory considering these boundary conditions (upper curves in Figure 4). For the studied configurations, the effect of the

amplitude of imperfections and of the boundary conditions on the minimum buckling load is equal to 13% and 17%, respectively. The effect of boundary conditions is reduced (expected 70% from Figure 4) due to imperfections.

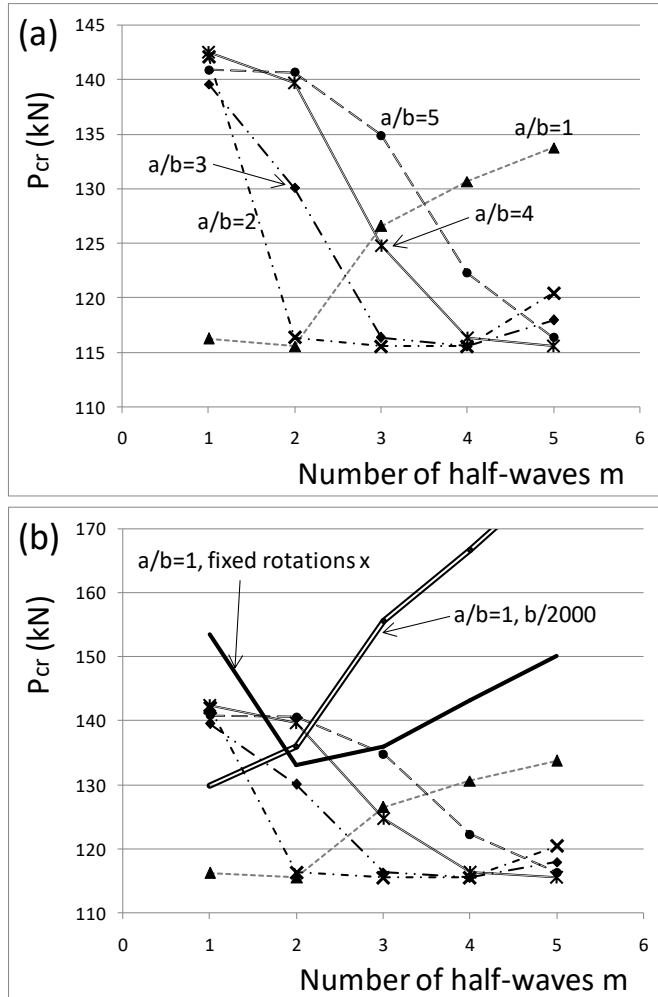


Figure 8. Parametric analysis results for stiffened (web) plate (S235, 550 °C) (a) effect of a/b and m on the critical load and (b) effect of imperfection amplitude and boundary conditions.

The analysis results for the unstiffened plate (flange) are presented in Figure 9. Two different slenderness are studied. Figure 9(a) presents the results for plates with $\lambda_{p,\theta}$ equal with 1.0 (intermediate slenderness). It can be seen that the minimum buckling load is obtained for $a/b > 3$ and $m = 1$. When the plate is slender ($\lambda_{p,\theta} = 2.0$, Figure 9(b)), the minimum occurs for $a/b > 4$ and $m > 3$. For unstiffened plates, it is important to know whether the behaviour is the one of an intermediate slenderness plate (i.e. Figure 9(a)) or of a slender plate (Figure 9(b)). Indeed, adopting $a/b > 3$ and $m=1$ for a slender plate leads to an overestimation of 28% of the buckling load,

compared to the minimum value (which is obtained for $a/b > 4$ and $m > 3$). Conversely, adopting $a/b > 4$ and $m > 3$ for an intermediate slenderness plate results in an overestimation of 15 % of the minimum buckling load. From parametric analyses it is found that this change happens around a slenderness value of $\lambda_{p,\theta} = 1.2$, which is compatible with Figure 5c. As the buckling mode is not compatible with the applied imperfections of $a/b > 4$ and $m > 3$, the critical force is higher at intermediate slenderness. But for $\lambda_{p,\theta} > 1.2$, these imperfection shapes are giving minimum post-buckling response.

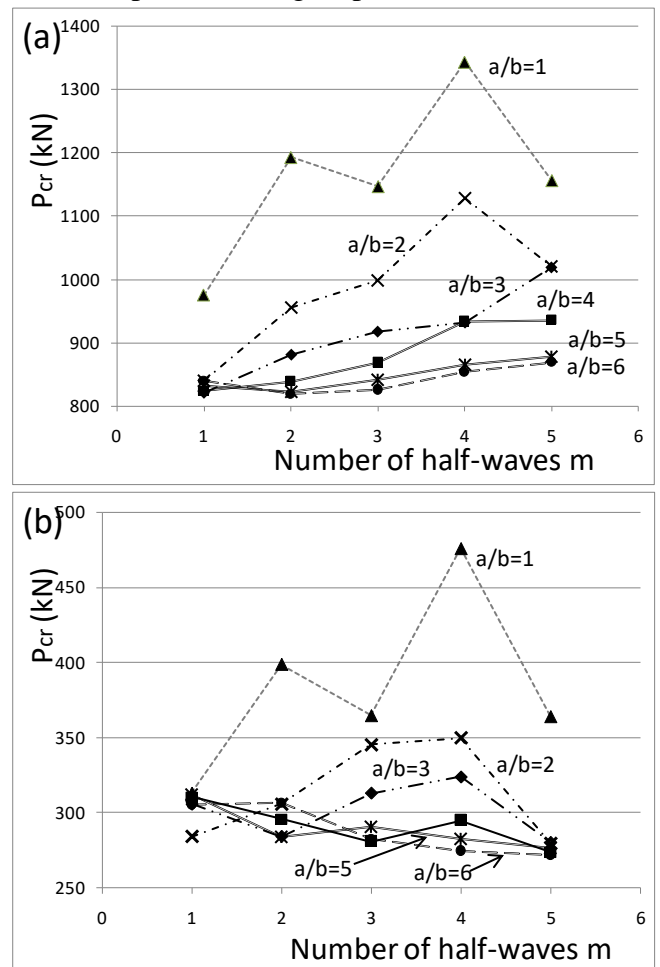


Figure 9. Parametric analysis results for unstiffened (flange) plate (S235, 550 °C) (a) for $\lambda_{p,\theta} = 1.0$ and (b) $\lambda_{p,\theta} = 2.0$.

When $a/b = 1$, the critical load is high as expected from the perfect plate theory. From Figure 9, it is clear that the critical load of the square plate is also affected by the odd or even number of half-waves. This happens because initially applied imperfections following an even number of half waves are incompatible with the natural tendency of the plate to buckle in one half wave. It should be noted that the isolated plate analysis method to simulate plated structural elements

relies on two simplifying assumptions. First, the boundary conditions applied on the studied plate are a simplification which ignores the actual stiffness of the other plates of the cross section. Second, the temperature is considered uniform, which might be inaccurate in structural applications. Yet, this method has been largely used by researchers to approximate the behaviour of thin plate structures. Consequently, it is important to study the effects of the parameters that affect the results and provide

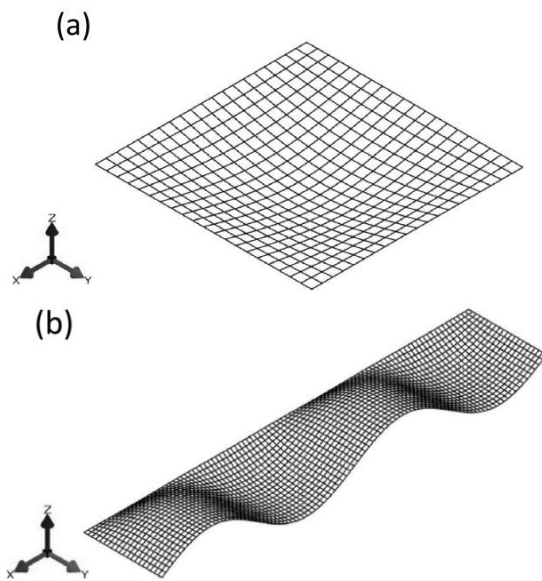


Figure 10. Failure modes of (a) four sides simply supported plate (web) with $a/b=1$ and $m=1$ and (b) three sides simply supported plate (flange) with $a/b=5$ and $m=4$.

6. CONCLUSIONS

From the presented analysis results in conjunction with the theoretical background presented in Sections 2 and 3, the following conclusions can be drawn:

- The buckling behaviour of real steel plates at elevated temperatures is complex, influenced by imperfections, and cannot be predicted from perfect plate theory alone.

- The finite element method can be used to simulate the buckling behaviour of steel plates at elevated temperatures. However, the results are strongly dependent on certain parameters (a/b , m , boundary conditions). Significantly unsafe results can be obtained from FEA for certain combinations of the parameters.

- For the analysis of stiffened plates (web), the use of rectangular plates with sides ratio a/b and a number m of half-waves of imperfections equal to

recommendations as regards the values to adopt to ensure that the results are on the safe side.

In terms of recommendation, a simplification for the isolated flange simulation could be the use of ($a/b > 4$, $m > 3$) for unstiffened (flange) plates and for all the range of slenderness. However, it must be kept in mind that this would result in an overestimation of the critical load for unstiffened plate of intermediate slenderness.

Typical failure modes are presented in Figure 10.

$m=a/b$ or $m=a/b+1$ is giving safe results (i.e. the minimum buckling load). The use of $a/b=m=1$ is proposed, as it giving safe results and the computational time is minimum.

- For the analysis of unstiffened plates (flange), the set of parameters leading to minimum buckling load depends on the slenderness ratio. Rectangular plates with sides ratio $a/b > 4$ should be used in any case, but the number of half-waves of imperfections leading to safe results is $m=1$ for $\lambda_{p,0} < 1.2$ and $m > 3$ for $\lambda_{p,0} < 1.2$.

- For the analysis of unstiffened plates (flange), the use of rectangular plates with sides ratio $a/b > 4$ and half-waves of imperfections $m > 3$ is proposed as a simplification but it is an unconservative assumption.

ACKNOWLEDGEMENTS

This research was supported by the University of Liege and the EU in the context of the FP7-PEOPLE-COFUND-BelIPD project.

REFERENCES

1. MCALLISTER, T., 2008. 'Federal building and fire safety investigation of the World Trade Center disaster: structural fire response and probable collapse sequence of World Trade Center building 7'. Gaithersburg, MD, National Institute of Standards and Technology [NIST NCSTAR 1-9].
2. WANG, Y.C., 2002. 'Steel and composite structures: behaviour and design for fire safety', CRC Press, London.
3. COUTO, C., REAL, P.V., LOPES, N., ZHAO, B., 2014. 'Effective width method to account for the local buckling of steel thin plates at elevated temperatures', Thin-Walled Structures, 84, p. 134-149.

4. COUTO, C., REAL, P.V., LOPES, N., ZHAO, B., 2015. 'Resistance of steel cross-sections with local buckling at elevated temperatures', *Constructional Steel Research*, 109, p. 101-104.
5. FRANSSEN, J.M., COWEZ, B., GERNAY, T., 2014. 'Effective stress method to be used in beam finite elements to take local instabilities into account'. *Fire Safety Science* 11, 544-557. 10.3801/IAFSS.FSS.11-544.
6. QUIEL, S.E., GARLOCK, M.E.M., 2010. 'Calculating the buckling strength of steel plates exposed to fire', *Thin-Walled Structures*, 48, p. 684-695.
7. KNOBLOCH, M., FONTANA, M., 2006. 'Strain-based approach to local buckling of steel sections subjected to fire'. *Constructional Steel Research*, 62, p. 44-67.
8. EN 1993-1-5, 2006. 'Eurocode 3 — design of steel structures — part 1-5: plated structural elements'. Brussels: European Committee for Standardisation.
9. AISC, 2005. 'Steel construction manual', 13th ed. American Institute of Steel Construction.
10. EN 1993-1-2, 2005. 'Eurocode 3: design of steel structures — part 1-2: general rules — structural fire design'. Brussels: European Committee for Standardisation.
11. GERALD, G, BACKER, H. 'Buckling of Flat Plates', NACA Technical Note 3781, USA, 1957.
12. MARAVEAS, C., GERNAY, T., FRANSSEN, J.M., 2017. 'Sensitivity of elevated temperature load carrying capacity of thin-walled steel members', *Applications of Structural Fire Engineering (ASFE'17)*, Manchester, UK.
13. BRUSH, D.O. and ALMROTH, B.O., 1975, 'Buckling of Bars, Plates and Shells', McGraw-Hill Kogakusha, USA.
14. STRUCTURAL STABILITY RESEARCH COUNCIL, 2009, Chapter 4: Plates, USA.
15. YU, C., and SCHAFER, B. W. 2007. 'Effect of longitudinal stress gradients on elastic buckling of thin plates' *Journal of Engineering Mechanics*, 133(4), 452-463.
16. STIEMER, S.F., CIVL432 Advanced Structural Steel Design Lecture Notes, University of British Columbia, Canada.
17. FRANSSEN, J.-M., 2005. 'SAFIR, A thermal/Structural Program for Modelling Structures under Fire', *Eng J A.I.S.C.*, 42, p. 143-158.
18. FRANSSEN, J.M., and GERNAY, T., 2017. 'Modeling structures in fire with SAFIR®: Theoretical background and capabilities', *Journal of Structural Fire Engineering*, 8(3).
19. FIDESC4, 2015, 'Fire design of steel members with welded or hot-rolled class 4 cross-sections', Final report, Research program of the Research Fund for Coal and Steel.